Pergamon

0301-9322(95)00088-7

Int. J. Multiphase Flow Vol. 22, No. 3, pp. 417–429, 1996

0301-9322/96 $15.00 + 0.00

PRESSURE WAVES IN A LIQUID SUSPENSION WITH SOLID PARTICLES AND GAS BUBBLES

V. E. NAKORYAKOV, V. E. DONTSOV and B. G. POKUSAEV
Institute of Thermophysics of the Siberian Branch of RAS, Novosibirsk-90, 630090, Russia

(Received 25 May 1994; in revised form 19 December 1995)

Abstract—The evolution and structure of pressure waves of moderate intensity in a liquid suspension with solid particles and gas bubbles were investigated experimentally. The experimental data was generalized on the basis of theoretical relations. It was shown that dispersive and non-linear effects significantly affect wave dynamics. Copyright © 1996 Elsevier Science Ltd.

Key Words: three-phase medium, liquid suspension with solid particles, gas bubbles, pressure waves

1. INTRODUCTION

The pressure disturbance propagation in a liquid suspension with solid particles has been extensively investigated by many authors. In paper of Kuster & Toksoz (1974), and Mehta (1983) the relations for a wave velocity and acoustic wave attenuation coefficient were obtained on the basis of multiple scattering theory and comparison with experimental data was carried out. Considering Biot's model for a sound propagation in saturated porous media, Hovem (1980) obtained a close agreement between the theory and the experimental data for a velocity field and sound attenuation in suspensions. Space-averaged equations for mechanics of heterogeneous media were derived by Nigmatulin (1978). This set of equations allows us the consideration of wave evolution in two-phase medium. Numerous theoretical and experimental investigations on the wave dynamics in gas–liquid media has been performed by Nakoryakov *et al.* (1983). Wave propagation in porous medium filled by gas–liquid mixture has been studied by Dontsov (1992).

The aim of the present paper is to investigate experimentally the evolution and structure of pressure waves of moderate intensity in a liquid suspension with solid particles and gas bubbles (three-phase medium). Experimental data were considered in a framework of performed theoretical analysis.

2. THEORETICAL ANALYSIS

Propagation of one-dimensional pressure disturbances in a three-phase medium (liquid, solid balls, and gas bubbles) was considered assuming the wavelength to be much larger than the sizes of balls and gas bubbles as well as the distances between them. The liquid with the gas bubbles will be considered as a homogeneous medium with average density ρ_m, pressure p and velocity v_m. We propose that the following conditions are fulfilled: (a) solid particles are spherical with a same diameter; (b) there is no collisions between solid particles and there is neither destruction nor formation of new solid particles or bubbles. The set of equations which describes a one-dimensional pressure disturbance propagation in dispersed medium takes the form (Nigmatulin 1978):

$$\frac{\partial \phi \rho_m}{\partial t} + \frac{\partial (\phi \rho_m V_m)}{\partial x} = 0$$

$$\frac{\partial (1-\phi)\rho_l}{\partial t} + \frac{\partial (1-\phi)\rho_l V_l}{\partial x} = 0 \qquad [1]$$

$$\alpha\phi\rho_m\frac{\partial V_m}{\partial t}-(\alpha-1)\phi\rho_m\frac{\partial V_1}{\partial t}=-\phi\frac{\partial p}{\partial x}-F_\mu-(\alpha-1)\phi\rho_m\frac{\partial V_m}{\partial t}$$

$$+((1-\phi)\rho_1+(\alpha-1)\phi\rho_m)\frac{\partial V_1}{\partial t}=-(1-\phi)\frac{\partial p}{\partial x}+F_\mu,\ \rho_1=\text{const},$$

where $\rho_m=\rho_2(1-\epsilon)+\rho_3\epsilon$, ϕ is the medium porosity, ϵ is the volume gas content in liquid. The quantity $\phi\epsilon$ corresponds to the volume gas content in a three-phase medium provided the value of ϵ small enough; α is the added liquid mass coefficient. The subscripts denote the following: (1) the solid phase, (2) the liquid phase, (3) the gas phase, (m) the gas–liquid mixture. The index 0 corresponds to the initial phase state.

The interface force F_μ (Nigmatulin 1978) is:

$$F_\mu=\frac{3}{4}\frac{c_\mu\rho_m\phi(1-\phi)(V_m-V_1)^2}{d}$$

where d is the solid balls diameter, c_μ is the coefficient of resistance which should be determined from the experiment. For small values of relative velocity the interface force depends linearly on relative velocity and may be represented by:

$$F_\mu=\frac{\phi^2\nu\rho_m}{K_0}(V_m-V_1)$$

where K_0 is the permeability of the medium which is usually introduced for porous media study, ν is the kinematics viscosity of a liquid.

In order to close the set of equations [1] we will derive the relationship between pressure p and the homogeneous mixture density ρ_m, using the equation for single bubble pulsations in a liquid with suspended solid particles. We assume that (a) the number of bubbles in per unit volume of medium is constant and bubbles obey adiabatic law; (b) gas bubbles are spherical; they have identical size and the bubble's oscillation has a small amplitude.

Let us consider the two limiting cases for bubble pulsations.

High frequency limit

In the first limiting case, when liquid and solid balls densities are quite different and the bubble's pulsation frequency is high ($\omega\gg\omega_\nu=\phi\nu/20K_0$—Nakoryakov *et al.* 1989) the solid balls do not have enough time to be involved in radial motion near a bubble. In this case the equation for bubble pulsations will be identical to that for the bubble oscillations in a incompressible porous medium (Nakoryakov *et al.* 1989). Substituting again the bubble radius by the mixture density ρ_m we obtain the following equation:

$$\delta\left(\rho_m-\frac{p}{c_0^2}\right)=-\frac{1}{c_0^2}\left(\beta\frac{\partial^2\rho_m}{\partial t^2}+\frac{4\nu^*}{3\epsilon}\frac{\partial\rho_m}{\partial t}+Bc_0^2(\delta\rho_m)^2\right)\qquad[2]$$

where $c_0=(\gamma p_0/\rho_m\epsilon)^{0.5}$ is the low-frequency ($\omega\leqslant\omega_0$) sound velocity in a gas–liquid mixture, $B=(\gamma+1)/2\rho_m\epsilon$, $\nu^*=\nu(1+\phi R_0^2/4K_0)+\nu_t$, $\beta=R_0^2/3\epsilon$, $\nu_t=(\gamma-1)R_0^2(\omega_0 a)^{0.5}/\sqrt{2}\epsilon$ is the coefficient of the effective thermal viscosity (Nakoryakov *et al.* 1983); ω_0 is the resonant frequency of bubble pulsations, a is the gas temperature conductivity coefficient, R_0 is the bubble radius, γ is adiabatic index.

Our goal is to derive from the closed set [1] and [2] the evolution equation for the pressure p supposing that non-linear, discursive and dissipative terms of equation are small. Since the nonlinearity in equation [2] significantly exceeds the hydrodynamic non-linearity in [1] one is able to linearize the set [1]. Assuming a linear dependence of the interface force (liquid–solid balls) on their relative velocity and taking into account the nonstationary Basset's force (Nigmatulin 1978), we can reduce the system [1] to the equation

$$\frac{\partial^2\rho_m}{\partial t^2}-\left(\frac{c}{c_0}\right)^2\frac{\partial^2 p}{\partial x^2}+\frac{\phi\nu}{K_0}\frac{\phi(1-\phi)\rho_1-((c_0/c)^2-\phi^2)\rho_m}{\alpha\phi(1-\phi)\rho_1+(\alpha-1)\phi^2\rho_m}$$

$$\times\left(\frac{\partial\rho_m}{\partial t}+\frac{1}{(2\pi\phi\nu/20K_0)^{0.5}}\int_0^t\frac{\partial\rho_m}{\partial\tau}\frac{d\tau}{(t-\tau)^{0.5}}\right)=0\qquad[3]$$

where

$$c = c_0\left(\frac{(\alpha - 2\phi + \phi^2)\rho_m + \phi(1-\phi)\rho_l}{\alpha\phi(1-\phi)\rho_l + (\alpha-1)\phi^2\rho_m}\right)^{0.5}$$

is the low-frequency ($\omega_v \leqslant \leqslant \omega \leqslant \omega_0$) sound velocity in a three-phase medium (the low-frequency velocity of small pressure perturbations).

Assuming that nonlinear, dispersion and dissipation terms are small and substituting $\delta\rho_m = \delta p/c_0^2$ from [2] and [3] one obtains the following evolution equation:

$$\frac{\partial^2 p}{\partial t^2} - c^2\frac{\partial^2 p}{\partial x^2} + \frac{\phi\nu}{K_0}\frac{\phi(1-\phi)\rho_l - ((c_0/c)^2 - \phi^2)\rho_m}{\alpha\phi(1-\phi)\rho_l + (\alpha-1)\phi^2\rho_m} \times \left(\frac{\partial p}{\partial t} + \frac{1}{(2\pi\phi\nu/20K_0)^{0.5}}\int_0^t \frac{\partial p}{\partial \tau}\frac{d\tau}{(t-\tau)^{0.5}}\right) - \left(\frac{c}{c_0}\right)^2\left(\beta\frac{\partial^4 p}{\partial x^2\,\partial t^2} + \frac{4\nu^*}{3\epsilon}\frac{\partial^3 p}{\partial x^2\,\partial t} + B\frac{\partial^2(\delta p)^2}{\partial x^2}\right) = 0. \quad [4]$$

Ignoring the added liquid mass the expression for sound velocity has the form:

$$c^* = c_{/\alpha=1} = \left(\frac{\gamma p_0}{\rho_m\epsilon}\left(1 + \frac{1-\phi}{\phi}\cdot\frac{\rho_m}{\rho_l}\right)\right)^{0.5}$$

The equation obtained differs from the Navier–Stokes–Bussinesque equation for bubble systems by the additional term corresponding to the viscous dissipation caused by the longitudinal relative movement of liquid and solid particles in a wave. Ignoring dissipation one is able to obtain the following solution in the form of a shock wave with velocity (Nakoryakov *et al.* 1980):

$$\frac{U}{c} = \left(1 + \frac{\gamma+1}{2\gamma}\frac{\delta p}{p_0}\right)^{0.5}. \quad [5]$$

Neglecting all dissipate losses in [4] we will obtain the Bussinesque's equation which has the stationary solutions in a form of solitons. The expressions for the velocity of a soliton and its half-width are as follows (Nakoryakov *et al.* 1980):

$$\frac{U_s}{c} = \left(1 + \frac{\gamma+1}{3\gamma}\frac{\delta p_m}{p_0}\right)^{0.5}$$

$$\delta_c = \left(\beta\left(4 + \frac{12p_0}{\delta p_m}\frac{\gamma}{\gamma+1}\right)\right)^{0.5}\left(\frac{c}{c_0}\right). \quad [6]$$

If $\epsilon \to 0$ we obtain two-phase medium (a liquid suspension with solid particles, $c_0 \to c_2$, $\rho_m \to \rho_2$). Following [3] the expression for high-frequency sound velocity in two-phase medium is:

$$\bar{c} = c_2\left(\frac{(\alpha - 2\phi + \phi^2)\rho_2 + \phi(1-\phi)\rho_l}{\alpha\phi(1-\phi)\rho_l + (\alpha-1)\phi^2\rho_2}\right)^{0.5} \quad [7]$$

where c_2 is the sound velocity in a liquid. This expression corresponds to a high frequency limit of sound velocity in fluid saturated porous media if $K_s \to \infty$, $K_B = N = 0$ (Johnson & Plona 1982). K_s, K_B, and N are the bulk modules of solid, porous skeleton and the shear module of porous skeleton, respectively.

Low frequency limit

There is no relative radial movement between the liquid and the solid particles in this case, i.e. the particles are frozen in the liquid. We obtain well known Rayleigh equation for bubble pulsations in liquid with an effective density $\rho_0 = \rho_l(1-\phi) + \rho_2\phi$. This approach is valid for both cases: (a) densities of the liquid and solid phase are close; (b) period of bubble pulsation is longer than the characteristic time of the developing of a liquid boundary layers on the solid balls.

Following the ideas of Nakoryakov's paper (1983) on dynamics of waves in the gas–liquid media and substituting the bubble radius by the three-phase media density ρ it can be written as

$$(\rho = \rho_0(1 - \epsilon\phi) + \rho_3\epsilon\phi)$$

$$\delta\left(\rho - \frac{p}{c_e^2}\right) = -\frac{1}{c_e^2}\left(\bar{\beta}\frac{\partial^2 \rho}{\partial t^2} + \frac{4\bar{\nu}}{3\epsilon\phi}\frac{\partial \rho}{\partial t} + \bar{B}c_e^2(\delta\rho)^2\right) \quad [8]$$

where $c_e = (\gamma p_0/\rho\epsilon\phi)^{0.5}$ is the low frequency sound velocity in a three-phase medium (equilibrium velocity), $\bar{\beta} = R_0^2/3\epsilon\phi$ is the dispersion coefficient, $\bar{B} = (\gamma + 1)/2\rho\epsilon\phi$ is the nonlinearity coefficient, R_0 is the bubble radius, $\bar{\nu}$ is the effective viscosity coefficient of suspension of liquid and solid particles.

Using [8] and the momentum equations for equilibrium three-phase medium we obtain the evolution equation for a low-frequency limit:

$$\frac{\partial^2 p}{\partial t^2} - c_e^2\frac{\partial^2 p}{\partial x^2} - \bar{\beta}\frac{\partial^4 p}{\partial x^2 \partial t^2} - \frac{4\bar{\nu}}{3\epsilon\phi}\frac{\partial^3 p}{\partial x^2 \partial t} - \bar{B}\frac{\partial^2 (\delta p)^2}{\partial x^2} = 0. \quad [9]$$

Neglecting the dissipative losses we obtain a stationary solution in a form of solitons (Nakoryakov *et al.* 1980):

$$\Delta p = \delta p_m \sec h^2\left(\frac{x}{\delta_c}\right), \quad \delta_c = \left(\bar{\beta}\left(4 + \frac{12p_0}{\delta p_m}\right)\frac{\gamma}{\gamma + 1}\right)^{0.5}. \quad [10]$$

For a two-phase medium ($\epsilon = 0$, $c_0 = c_2$, $\rho_m = \rho_2$) the expression of sound velocity in low-frequency limit following [8] is

$$\bar{c}_e = c_2(\rho_2/\rho\phi)^{0.5}. \quad [11]$$

This expression is corresponded to Wood's formula with $K_s \to \infty$ (Johnson & Plona 1982).

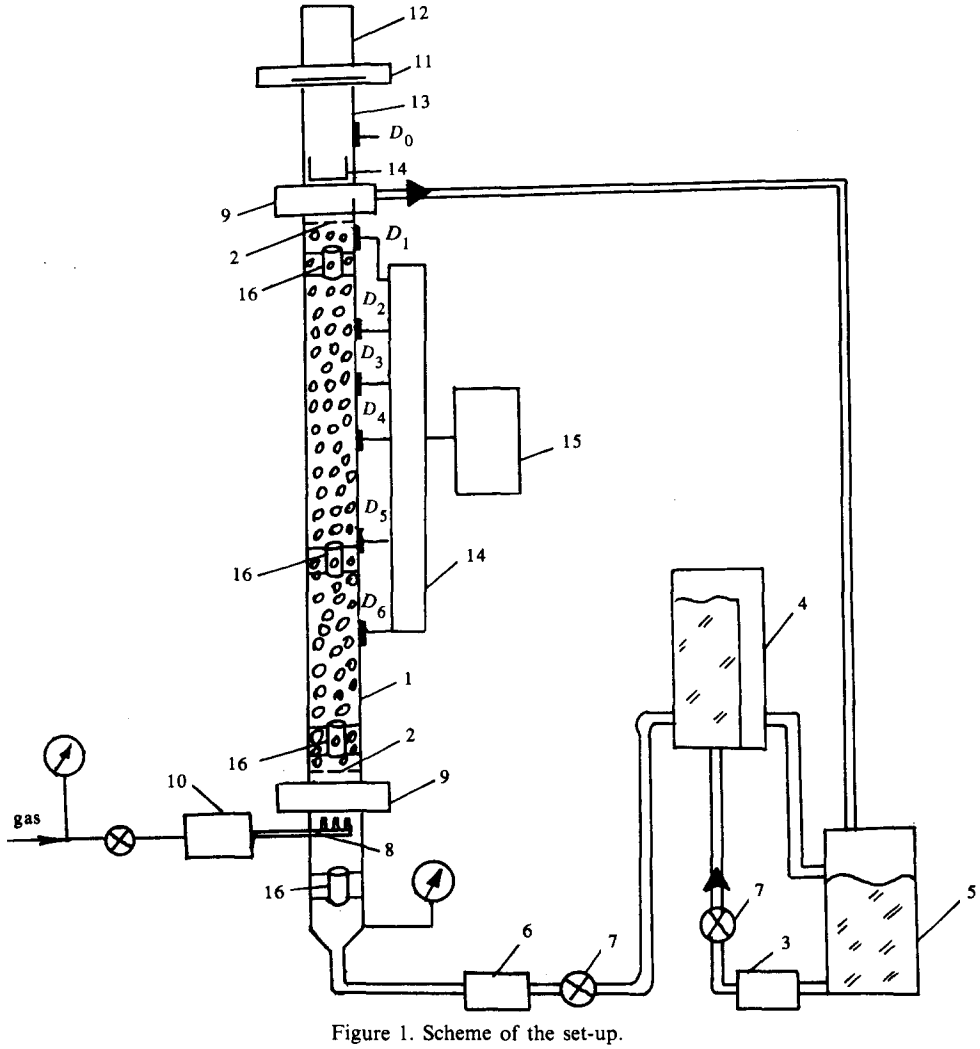

Figure 1. Scheme of the set-up.

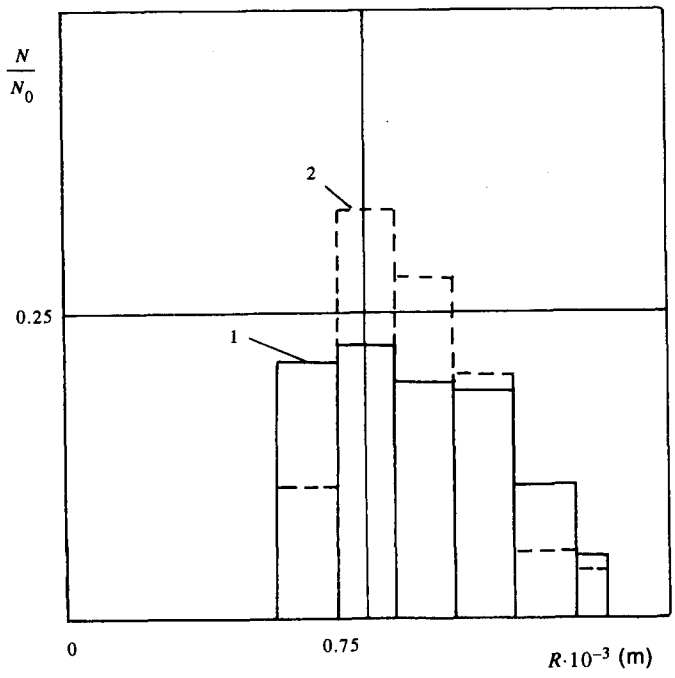

Figure 2. Histogram of air bubbles distribution in sizes. (1) $\epsilon = 2.3\%$; (2) $\epsilon = 0.85\%$.

3. EXPERIMENTAL SETUP AND PROCEDURE

To investigate pressure wave propagation in three-phase media (liquid–suspended solid particles–gas bubbles) we designed experimental setup which is shown in figure 1. The test section (1) is a vertical steel tube with an inner diameter of 0.052 m and a length of 1.5 m. The test section was partially filled with glass balls of 0.003 m diameter and was limited in the upper and lower parts by grids (2) with a 0.0025 m mesh. The porosity of the medium was determined according to a volume of the working section and the volume of the balls filling the section. To keep solid particles suspended, a liquid was pumped over the working section with a constant speed. For this purpose we used a system of a constant level which consisted of a pump (3), a tank of a constant level (4), a draining tank (5), an inductive liquid flow rate-meter (6), and regulating valves (7). Water and a water–glycerine solution were used as working liquids. Gas bubbles were introduced into a liquid at the bottom part of the working section through needle generator (8). Air and helium were used in experiments. A histogram of the air bubble propagation in sizes for two values of the gas contents is shown in figure 2. Here N_0 is all measured bubbles ($N_0 = 100\%$). N is a number of bubbles with a size in the range of $(R - R + \delta R)$. Bubble size was measured photographically. To take pictures of gas bubbles, we placed transparent windows (9) in the upper and bottom parts of the test section. Measurement of small gas flow rates was conducted by means of difference pressure gauge on a thin long capillary built into the gas supply system. A gas flow ratemeter (10) and a liquid flow ratemeter were previously calibrated.

A pressure wave with a step-like form was generated by a rupture of a diaphragm (11) that separates two chambers with high (12) and low (13) pressure, and then propagated through a light movable piston into the working section. To measure pressure wave profiles we used piezoelectric pressure sensors which were placed along the length of the working section and flush-mounted with its inner wall. Signals from the sensors were fed to ADC (14) and then processed by computer (15).

To measure small volume gas contents in a three-phase medium we used circular conductivity sensors (16) which were placed in the bottom, middle and upper parts of the working section. To reduce the influence of temperature change and a salt content in the water, we used a reference conductivity sensor, with was placed in front of the working section. The bridge scheme of measurement operates with a frequency of 1 kHz. The calibration of conductivity sensors was carried out in a two-phase (liquid–solid suspended particles) medium by means of small porosity

changes (1–5)% near the working value of porosity ϕ_0. The calibration curve is the time-averaged disbalance of bridge voltage on the relative porosity change $\delta\phi/\phi_0$. In a three-phase medium (gas bubbles/liquid/solid balls) we obtained a dependence of the gas flow rate on the averaged indicated value of bridge unbalance for the given working value of porosity. Finally, we built a calibrating dependence of the gas content $\epsilon = -\delta\phi/\phi_0$ on the gas flow rate at the given ϕ_0, which was used further in the experiment. The advantage of the given calibration method is the possibility to measure a rather small volume gas content ($\epsilon \leqslant 1\%$) by means of linear approximation of calibrating dependence to zero.

4. RESULTS OF EXPERIMENTS

The performed experiments reveal that nonlinear and dispersive effects significantly influence a wave propagation in a suspension of liquid, solid particles and gas bubbles. In figure 3 there is shown the evolution of a step-like profile wave in water with glass balls and air bubbles for different volume gas contents ϵ and wave intensities Δp. Here x is a distance from the entry of a wave into the medium up to the point of measurement. It is seen that for small values of ϵ and for small amplitude waves the dispersive and nonlinear effects are weak and, actually, do not change the shape of the wave, and the oscillating shock wave front can not be formed at considered distances (figure 3(a)). With wave amplitude increasing up to $\Delta p/p_0 \approx 1$, even at distance $x = 0.712$ m a quasi-stationary oscillating shock wave forms which, due to the dissipative processes, weakly attenuates as it propagates—see figure 3(b). As the gas volumetric content increases, the dissipation results in the appearance of the relaxation zone on the forward front of the wave and in the attenuation of oscillations—figure 3(c). Comparing these pressure wave profiles with results on the pressure wave propagation in gas–liquid media (Nakoryakov *et al.* 1983) we can remark their qualitative similarity. Thus, the introduction of a solid phase into a gas–liquid medium arises some quantitative changes into wave propagation velocity and structure. To describe a

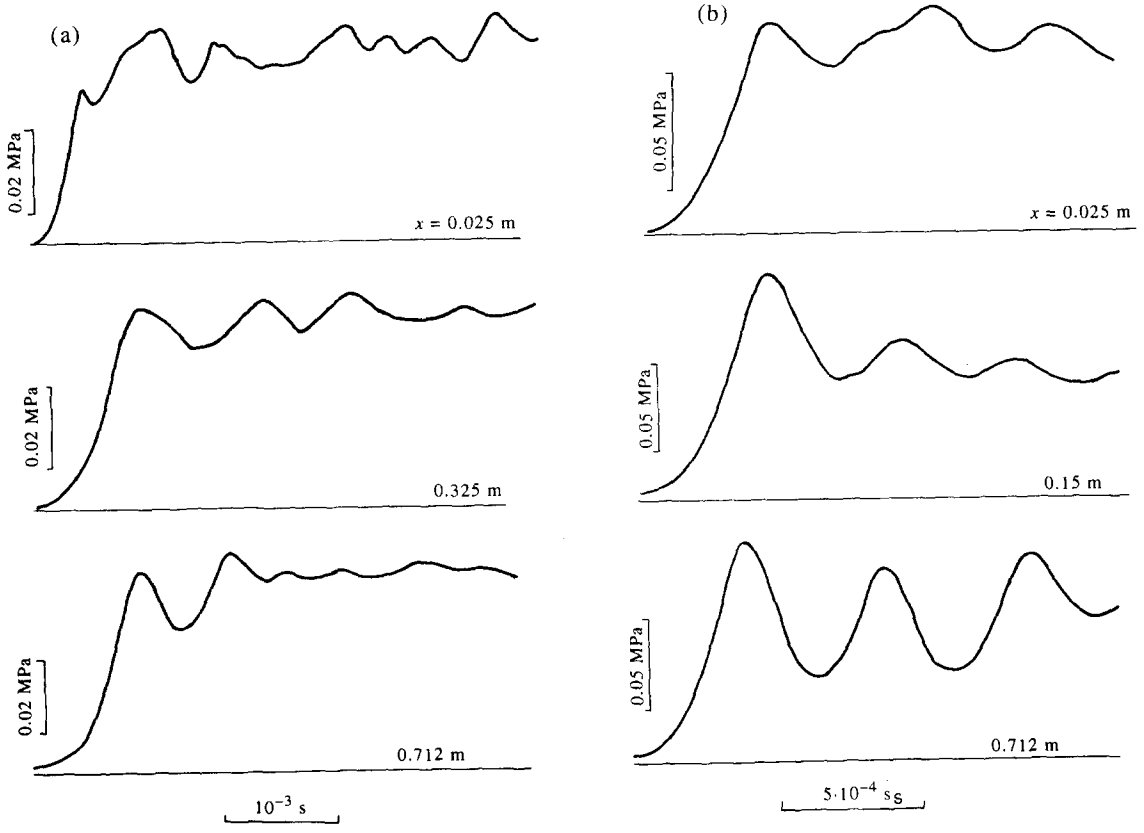

Figure 3(a, b). *(Caption opposite.)*

wave evolution in a three-phase medium more precisely, the solutions of [4] and [9] can be used.

To investigate the mechanisms of pressure wave attenuation in a three-phase medium, we used liquids with different viscosity: water and water–glycerine solution with viscosity of $\nu = 3 \times 10^{-6}\,m^2/s$. As well as gases with different thermal conductivity. It was shown that the pressure wave evolution in a water and in a water-glycerine solution (with solid balls and air bubbles in both cases) does not actually differ from the rest with similar parameters for a medium and a wave. However, a variation of a bubble gas thermal conductivity changes the dissipative properties of a medium. The pressure wave evolution patterns in a suspension of water with solid balls and gas bubbles (a—air, b—helium) are represented in figure 4. It is seen that the threehold increase of effective thermal viscosity coefficient accompanies the change of wave shape. The

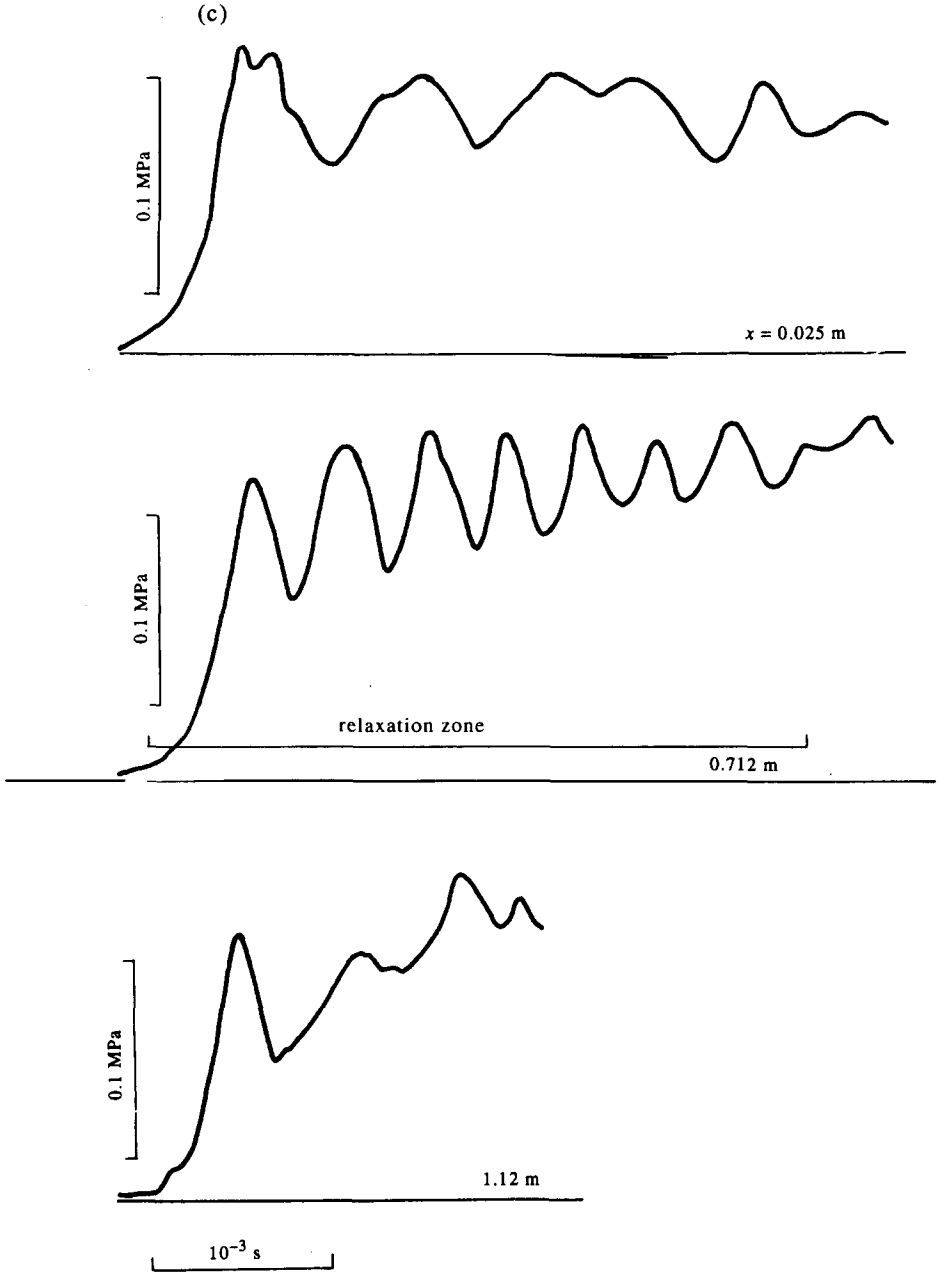

Figure 3. Evolution of a pressure wave of step-like profile in water with glass balls and air bubbles. $\phi = 0.58$, (a, b) $\epsilon = 0.5\%$; (c) $\epsilon = 2.3\%$.

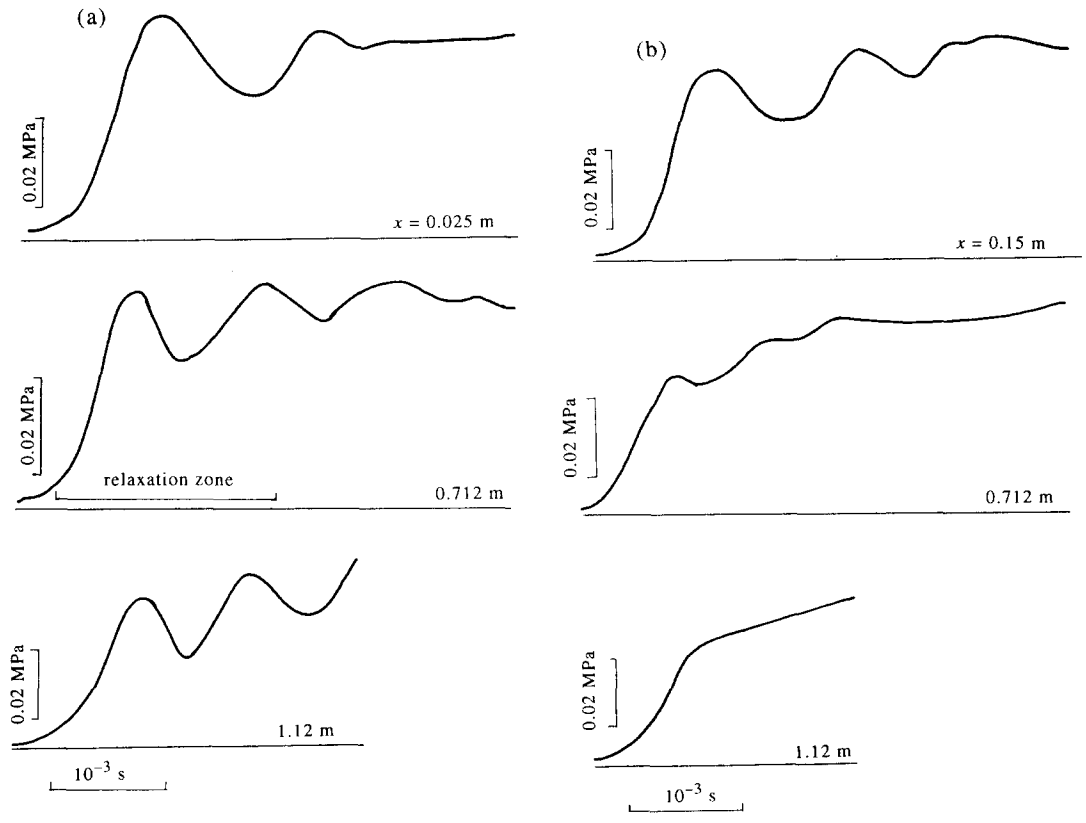

Figure 4. Evolution of a pressure wave in water suspension with glass balls and (a) air bubbles, (b) helium bubbles; $\phi = 0.58$, $\epsilon = 1.4\%$.

oscillating shock wave is depicted in figure 4(a); dissipative effects result only in the appearance of relaxation zone whereas in a medium with helium bubbles the monotonical profile without oscillations is formed (figure 4(b)). This is associated with enlargement of heat exchange between the gas in bubbles and their environment. Consequently, the main mechanism of wave dissipation in three-phase suspensions, as well as in gas–liquid media, is the thermal mechanism of dissipation.

The investigation on the structure of weak nonlinear oscillating shock waves shows that the first oscillation of a wave is properly described by a soliton form. The shape of shock wave (first oscillation only, curve 1) and calculated shape of wave (from [10]—curve 2; from [6]—curve 3) are shown in figure 5. Obviously, for wave amplitudes $\Delta p_m/p_0 \approx 1$ the experimental profile is

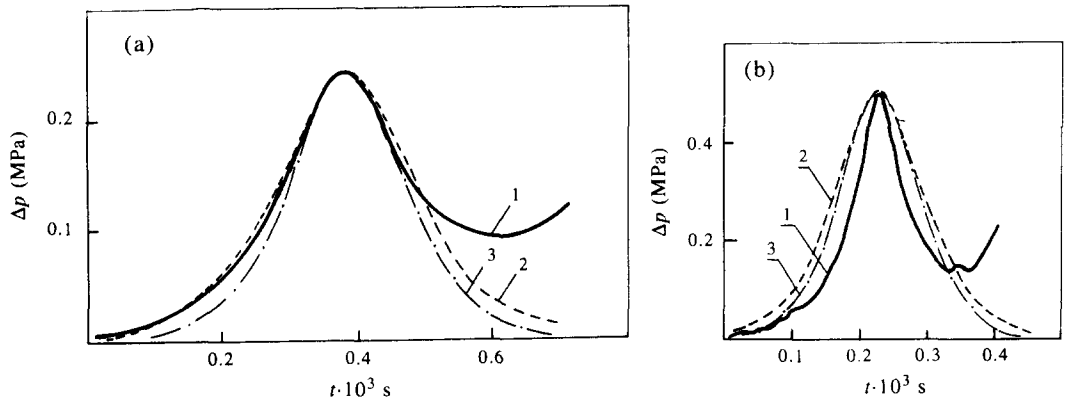

Figure 5. Shock wave shape (the first oscillation). (1) experiment; (2) calculation according to [10]; (3) calculation according to [6].

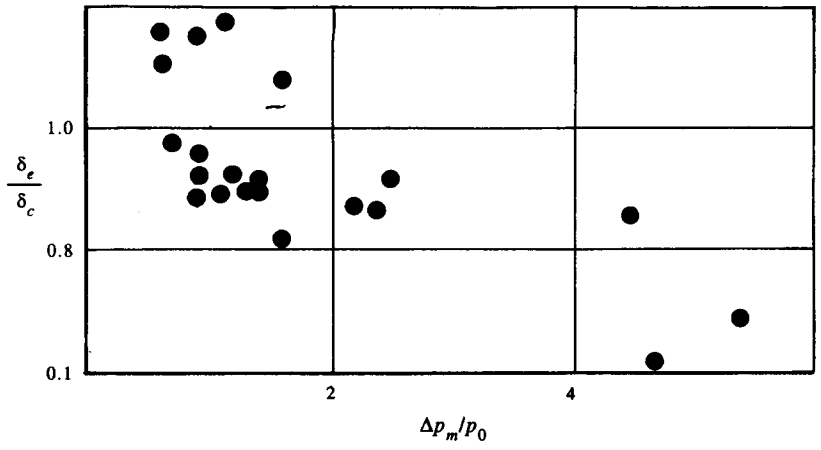

Figure 6. Half-width of a forward front of an oscillating shock wave.

properly approximated by the calculated curve 2 (figure 5(a)) which corresponds to model disregarding the relative radial movement of a liquid and the solid particles near bubbles in a wave. Thus, even for solid particles with rather high density ($\rho_1/\rho_2 = 2.46$), the dispersive properties of a three-phase medium do not actually differ from the dispersive properties of a gas–liquid medium. The medium dispersion coefficient is determined by the volume gas content in a three-phase medium $\epsilon\phi$ and is equal to $\bar{\beta} = R_0^2/3\epsilon\phi$.

With the increase of shock wave amplitude a significant decrease of oscillation duration and a sharpening of their shape takes place. An experimental profile of the first oscillation in the wave

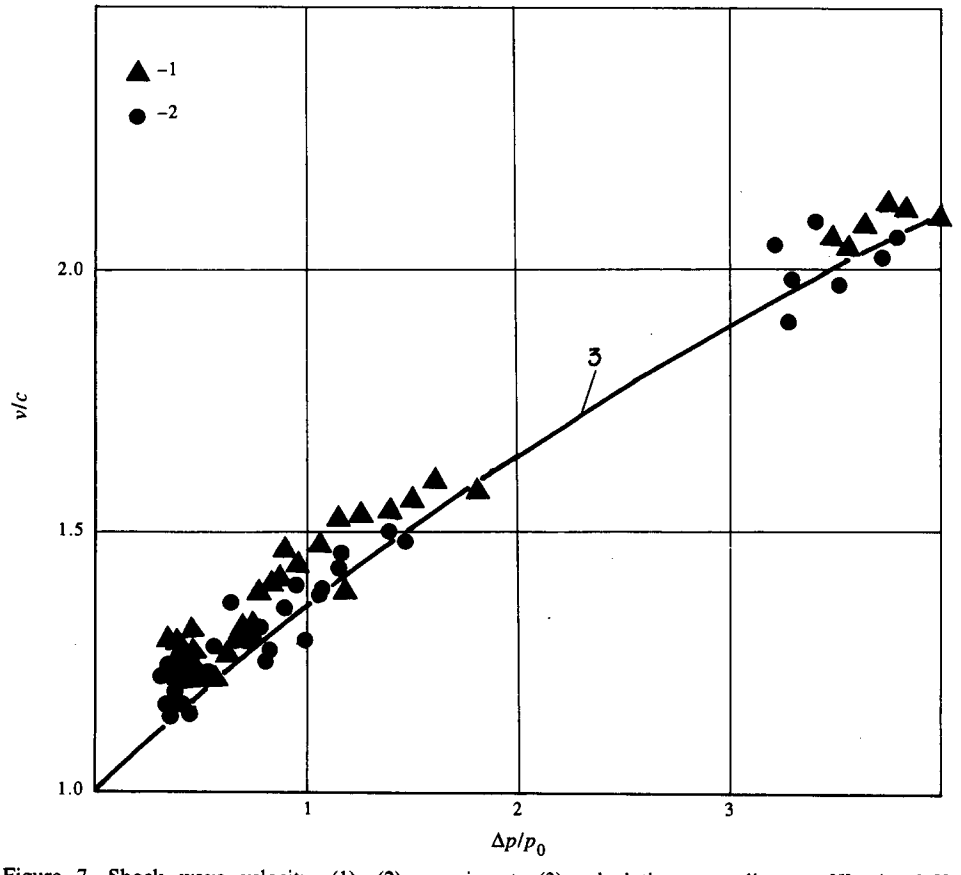

Figure 7. Shock wave velocity. (1), (2) experiment, (3) calculation according to [5], $\phi = 0.58$, $\epsilon = (0.5\text{–}2.5)\%$.

with an amplitude of $\Delta p_m/p_0 = 4.7$ (curve 1) differs from a shape of the calculated soliton (curve 2, [10]) and from curve 3 [6]—see figure 5(b).

A comparison of the half-width of the first wave oscillation δ_e observed in the experiments with that parameter from [10] (noted as δ_c) is shown in figure 6. Here, $\epsilon = (0.5\text{–}0.9)\%$. ($\delta_e = t^*U$, t^* is the time of pressure growth in a wave front from $0.42\Delta p_m$ to Δp_m, Δp_m is the amplitude of the first oscillation, U is a velocity of a shock wave.) If amplitudes $\Delta p_m/p_0 \leqslant 2$, the half-width of the first wave oscillation agrees with the calculated value of a soliton half-width. For a higher intensity ($\Delta p_m/p_0 \geqslant 2$) the experimental wave profile becomes significantly more narrow in comparison with calculated profile. A high scattering of experimental data is connected with a fairly wide distribution in bubble sizes and nonuniform distribution of bubbles along the tube length. A quasi-stationary property of the wave enhances this data scattering also.

Experimental data on the dependence of shock wave velocity in a three-phase medium on its amplitude are shown in figure 7. A water–air mixture was a working medium. The velocity (curve 1) measured on the initial part of propagation, coincides with the ones measured at a distance of 1 m from the entrance to the medium (curve 2). It suggests that a shock wave is formed immediately at the entrance to a three-phase medium. The calculated curve 3, derived according to [5], describes properly the experimental data within the investigated range of amplitudes. Thus, the inertial

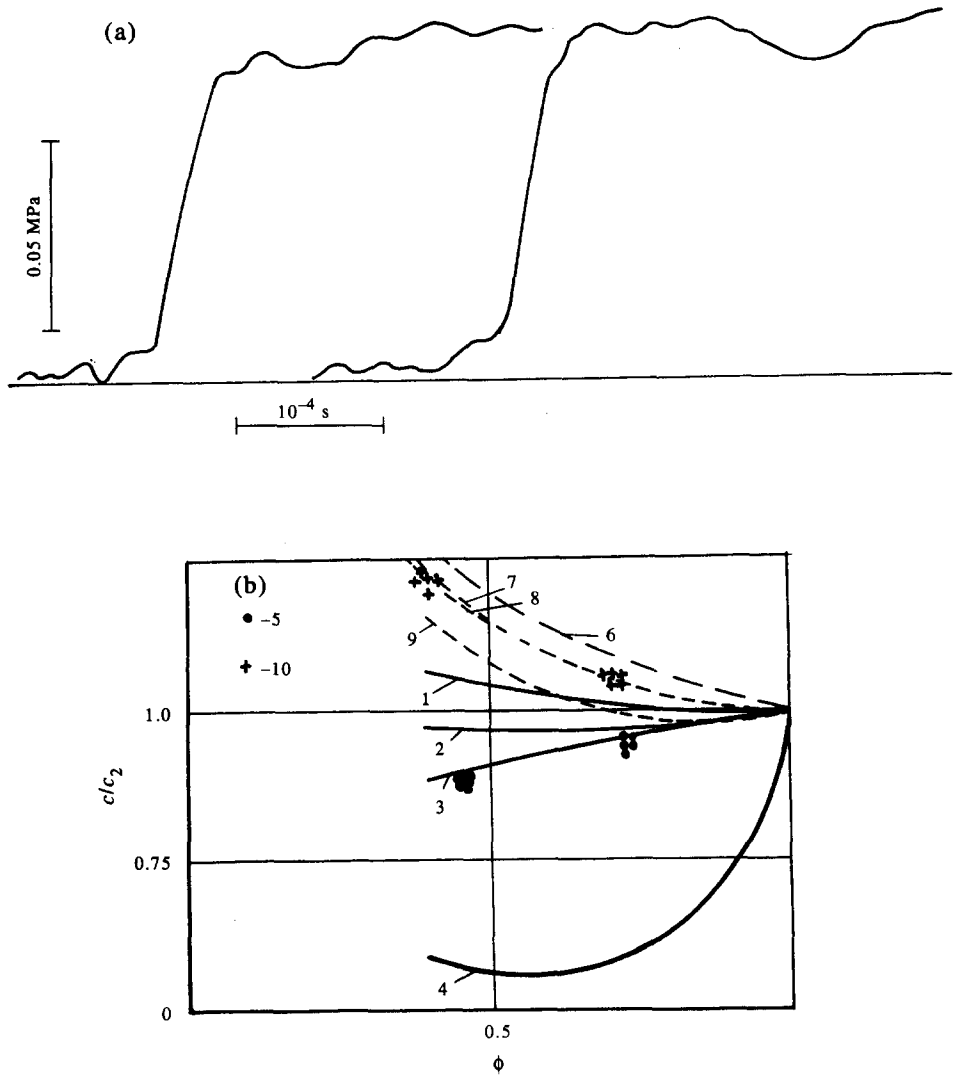

Figure 8. Sound velocity in a water suspension with (1–5) lead balls; glass balls (6–10). (5), (10) experiment (1–4), (6–9) calculations.

properties of the solid phase have a great influence on the velocity of wave propagation. A high-frequency limit and velocity c is more appropriate for calculation of shock wave velocity than the equilibrium velocity c_e. Note that the values of calculated velocity considering the added liquid mass $\alpha = 1 - 0.5(1 - 1/\phi)$ (Berryman 1980) and this velocity disregarding added mass effect ($\alpha = 1$) differs by 3% only, but this is less than the precision of measurement.

Let us discuss the influence of added liquid mass α on the velocity of wave propagation. To increase the precision, we carried out the measurements of a wave velocity in a suspension of a liquid with solid particles without gas bubbles. The characteristic profiles of pressure waves in a water suspension with lead balls are shown in figure 8(a). The calculated dependencies of sound velocities in a water suspension with lead balls (curves 1–4) and with glass balls (curves 6–9) on medium porosity are presented. Here c_2 is the sound velocity in a liquid measured directly during the experiment. The lines (1, 6) correspond to a high-frequency sound velocity [7] at $\alpha = 1$, curves 2, 7 describe a high-frequency sound velocity [7] at $\alpha = 1 + 0.5(1 - \phi)$ (Nigmatulin 1978; Sergeev & Wallis 1991), curves 3, 8—high-frequency sound velocity [7] at $\alpha = 1 - 0.5(1 - 1/\phi)$ (Berryman 1980), curves 4, 9—low-frequency sound velocity [11]. Here, the experimental points for lead balls (curve 5) and glass balls (curve 10) are also given. It is seen (especially for lead balls) that the experimental data are properly described by the calculated curves (3–8) which take into account the influence of the added liquid mass on the wave propagation velocity according to Berryman (1980).

5. CONCLUSIONS

(1) The evolution equations describing the propagation of the weak nonlinear waves in liquid with the gas bubbles and the solid particles has been derived. The stationary solutions of these equations such as shock waves and solitons have been obtained.

(2) The experimental data on the structure, velocity and attenuation of the shock waves in three-phase medium have been obtained. The generalization of the experimental data on the basis of theoretical considerations was carried out.

(3) The main mechanism for attenuation of the pressure waves in a three-phase medium was shown to be a heat exchange between the gas bubbles and surrounding liquid.

(4) It was supported experimentally that the coefficient of added liquid mass has essential influence on the propagation velocity of the pressure wave.

Acknowledgements—This research was sponsored by the National Science Foundation (Grant NRPI000) and Russian Fundamental Research Foundation (95-01-01407).

REFERENCES

Berryman, J. G. 1980 Elastic wave propagation in fluid-saturated porous media. *J. Acoust. Soc. Am.* **69,** 416–424.

Dontsov, V. E. 1992 Structure and dynamics of pressure disturbances of final amplitude in a porous medium, saturated by a liquid with gas bubbles. *Izv. Akad. Nauk SSSR* **1,** 80–85.

Hovem, S. M. 1980 Viscous attenuation of sound in suspensions and high-porosity marine sediments. *J. Acoust. Soc. Am.* **67,** 1559–1563.

Johnson, D. L. & Plona, T. S. 1982 Slow waves and the consolidation transition. *J. Acoust. Soc. Am.* **72,** 556–565.

Kuster, G. T. & Toksoz, M. N. 1974 Velocity and attenuation of seismic waves in two-phase media. 1–2. *Geophysics* **39,** 587–618.

Mehta, C. H. 1983 Scattering theory of wave propagation in a two-phase medium. *Geophysics* **48,** 1359–1370.

Nakoryakov, V. E. Pokusaev, B. G. & Schreiber, I. R. 1983 *Propagation of Waves in Gas- and Vapor–Liquid Media.* Institute of Thermophysics, Novosibirsk, Russia.

Nakoryakov, V. E., Kuznetsov, V. V. & Dontsov, V. E. 1989 Pressure waves in saturated porous media. *Int. J. Multiphase Flow* **15,** 857–875.

Nakoryakov, V. E., Schreiber, I. R. & Gasenko, V. G. 1980 Moderate-intensity waves in liquid with gas bubbles. In *Wave Processes in Two-Phase Media*, pp. 5–19. Inst. of Thermophysics, Novosibirsk, Russia.

Nigmatulin, R. I. 1978 *Background in Mechanics of Heterogeneous Media.* Nauka, Moscow (in Russian).

Sergeev, Y. A. & Wallis, G. B. 1991 Propagation of concentration density disturbances in an inertially coupled two-phase dispersion. *Int. J. Multiphase Flow* **17**, 697–703.

APPENDIX

Derivation of the Evolution Equation

Assuming a linear approach we obtain from the first and the second equations of system [1]:

$$\rho_m \frac{\partial \phi}{\partial t} + \phi \frac{\partial \rho_m}{\partial t} + \phi \rho_m \frac{\partial V_m}{\partial t} = 0 \qquad [A1]$$

$$-\rho_1 \frac{\partial \phi}{\partial t} + (1-\phi)\rho_1 \frac{\partial V_1}{\partial x} = 0. \qquad [A2]$$

Excepting $\partial\phi/\partial t$ from [A1] and [A2] we obtain:

$$\phi \frac{\partial \rho_m}{\partial t} + \phi \rho_m \frac{\partial V_m}{\partial x} + (1-\phi)\rho_m \frac{\partial V_1}{\partial x} = 0. \qquad [A3]$$

From the third and fourth equations of system [1] we obtain:

$$\phi \rho_m \frac{\partial V_m}{\partial t} + (1-\phi)\rho_1 \frac{\partial V_1}{\partial t} = -\frac{\partial p}{\partial x}. \qquad [A4]$$

Taking a derivative by t of [A3] and taking x-derivative of [A4] and excluding by turns $\partial^2 V_m/\partial x \partial t$ and $\partial^2 V_1/\partial x \partial t$ we obtain:

$$(1-\phi)(\rho_1 - \rho_m)\frac{\partial^2 V_1}{\partial x \partial t} + \frac{\partial^2 p}{\partial x^2} - \phi \frac{\partial^2 \rho_m}{\partial t^2} = 0 \qquad [A5]$$

$$(\rho_m^2 - \rho_m \rho_1)\frac{\partial^2 V_m}{\partial x \partial t} + \rho_m \frac{\partial^2 p}{\partial x^2} - \phi \rho_1 \frac{\partial^2 \rho_m}{\partial t^2} = 0. \qquad [A6]$$

Taking a derivative by x of the third equation of system [1] and considering [A3], [A5], [A6] we obtain:

$$\frac{\partial^2 \rho_m}{\partial t^2} - \left(\frac{c}{c_0}\right)^2 \frac{\partial^2 p}{\partial x^2} - \frac{\phi \nu (1-\phi)(\rho_m - \rho_1)}{K_0(\phi\alpha(1-\phi)\rho_1 + (\alpha-1)\phi^2\rho_m)}\left(\phi \frac{\partial \rho_m}{\partial t} + \rho_m \frac{\partial V_1}{\partial x}\right) = 0 \qquad [A7]$$

$$c = c_0 \left(\frac{(\alpha - 2\phi + \phi^2)\rho_m + \phi(1-\phi)\rho_1}{\alpha\phi(1-\phi)\rho_1 + (\alpha-1)\phi^2\rho_m}\right)^{0.5}.$$

Assuming dissipation is negligible we obtain from [A7]:

$$\frac{\partial^2 \rho_m}{\partial t^2} \approx \left(\frac{c}{c_0}\right)^2 \frac{\partial^2 p}{\partial x^2}. \qquad [A8]$$

This expression is necessary for displacing of $\partial^2/\partial t^2$ by $\partial^2/\partial x^2$ in small dissipative term of [A7]:

$$\frac{\partial V_1}{\partial x} = \int \frac{\partial^2 V_1}{\partial x\, \partial t}\, dt = \frac{-1}{(1-\phi)(\rho_m - \rho_1)} \int \left(\phi \frac{\partial^2 \rho_m}{\partial t^2} - \frac{\partial^2 p}{\partial x^2}\right) dt$$

$$= \frac{-1}{(1-\phi)(\rho_m - \rho_1)} \int \left(\phi \frac{\partial^2 \rho_m}{\partial t^2} - \left(\frac{c_0}{c}\right)^2 \frac{\partial^2 \rho_m}{\partial t^2}\right) dt$$

$$= \frac{-1}{(1-\phi)(\rho_m - \rho_1)} \left(\phi - \left(\frac{c_0}{c}\right)^2\right) \frac{\partial \rho_m}{\partial t}.$$

Inserting the expression $\partial V_1/\partial x$ into [A7] and considering a non-stationary Basset's force we obtain:

$$\frac{\partial^2 \rho_m}{\partial t^2} - \left(\frac{c}{c_0}\right)^2 \frac{\partial^2 p}{\partial x^2} + \frac{\phi \nu}{K_0} \frac{\phi(1-\phi)\rho_l - ((c_0/c)^2 - \phi^2)\rho_m}{\alpha\phi(1-\phi)\rho_l + (\alpha - 1)\phi^2 \rho_m} \times \left(\frac{\partial \rho_m}{\partial t} + \frac{1}{(2\pi\phi\nu/20K_0)^{0.5}} \int_0^t \frac{\partial \rho_m}{\partial \tau} \frac{d\tau}{(t-\tau)^{0.5}}\right) = 0. \quad [A9]$$

Assuming that nonlinear, dispersive and dissipative terms in [A9] and [2] are small we can substitute in these terms $\delta\rho_m \approx \delta p/c_0^2$ and obtain the evolution equation:

$$\frac{\partial^2 p}{\partial t^2} - c^2 \frac{\partial^2 p}{\partial x^2} + \frac{\phi \nu}{K_0} \frac{\phi(1-\phi)\rho_l - ((c_0/c)^2 - \phi^2)\rho_m}{\alpha\phi(1-\phi)\rho_l + (\alpha - 1)\phi^2 \rho_m} \times \left(\frac{\partial p}{\partial t} + \frac{1}{(2\pi\phi\nu/20K_0)^{0.5}} \int_0^t \frac{\partial p}{\partial \tau} \frac{d\tau}{(t-\tau)^{0.5}}\right) - \left(\frac{1}{c_0}\right)^2 \left(\beta \frac{\partial^4 p}{\partial t^4} + \frac{4\nu^*}{3\epsilon} \frac{\partial^3 p}{\partial t^3} + B \frac{\partial^2 (\delta p)^2}{\partial t^2}\right) = 0. \quad [A10]$$

Approximating $\partial^2 p/\partial t^2 \approx c^2 \partial^2 p/\partial x^2$ in third last terms of equation [A10] we obtain the evolution equation [4].